

# SIMULATION STUDIES FOR THE CONFINEMENT OF ANTIPROTONS FOR THE AEgIS EXPERIMENT\*

B. Rawat<sup>1,†</sup>, N. Kumar<sup>1</sup>, B. Rienäcker, C. Welsch<sup>1</sup>

Department of Physics, University of Liverpool, Liverpool, United Kingdom

<sup>1</sup>also at The Cockcroft Institute, Daresbury, United Kingdom

## Abstract

The AEgIS (Antimatter Experiment: Gravity, Interferometry and Spectroscopy) project, based at CERN's Antiproton Decelerator (AD) facility, has undergone significant enhancements, capitalizing on the increased quantity of colder antiprotons made available by the new Extra Low Energy Antiproton Ring (ELENA) decelerator. These improvements aim to create antihydrogen  $\bar{H}$  and enable a direct investigation into the impact of gravity on antihydrogen atoms. This exploration seeks to probe the Weak Equivalence Principle for antimatter. In AEgIS experiment, a series of circular ring electrodes and an axial magnetic field of 1T are utilized for the trapping of cold antiprotons which are initially trapped in a 5T trap. This contribution describes the design and optimization of the electrodes to generate a parabolic potential, to effectively traps the antiprotons. The behaviour of the trapped antiprotons is reproduced by simulating a spherical source under different bias voltage settings applied to the electrodes. The general layout of the AEgIS trap is shown, alongside suitable, electrode configurations, and results from electrostatic particle-in-cell code simulations carried out to optimize the confinement time of the antiprotons in absence of any vacuum contaminants.

## INTRODUCTION

The AEgIS (Antimatter Experiment: Gravity, Interferometry, Spectroscopy)[1-3] experiment is designed to investigate the effects of gravity on antihydrogen atoms. This experiment is significant because, while we understand how gravity affects matter, its influence on antimatter remains largely unexplored [4]. The primary goal is to determine whether antihydrogen falls downwards under gravity (like ordinary matter) or exhibits some different behaviour.

The process begins with antiprotons being produced and initially decelerated from 5MeV in AD (Antiproton Decelerator) and later to 100 keV in the ELENA[5] (Extra Low Energy Antiproton) ring. ELENA is a facility at CERN designed to slow down antiprotons to energies suitable for antimatter studies like AEgIS.

These antiprotons are then transported to the AEgIS experiment via a series of transfer lines as depicted in Figure 1. Upon arrival at AEgIS, the antiprotons undergo several crucial steps to further decrease their energy to a level

<sup>†</sup>bharat26@liverpool.ac.uk

\*This work is a part of the AEgIS collaboration supported by EPSRC under grant agreement EP/X014851/1.

where they can be effectively manipulated and studied. Once the antiprotons are sufficiently slowed down, they are then trapped in electrostatic traps. These traps use electric fields to confine the antiprotons. The low energy and confinement of the antiprotons are crucial for the next steps in the AEgIS experiment, which involve combining them with Rydberg Positronium atoms to create antihydrogen atoms. The behaviour of these antihydrogen atoms under the influence of gravity is then studied, which is the core objective of the AEgIS experiment.

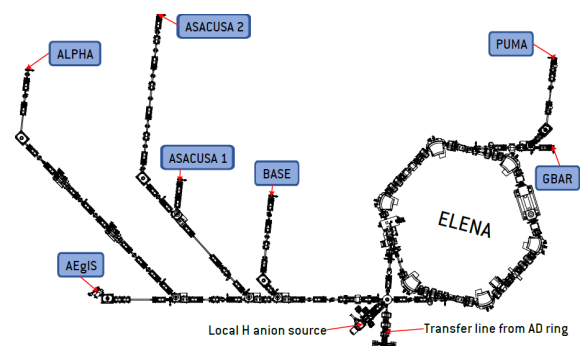


Figure 1: ELENA and its transfer lines

## SIMULATION SETUP

In the current study, we study the behaviour of cold antiprotons confined within the 1T region of the AEgIS experiment using a 3D electrostatic PIC simulation. Figure 2 presents 3D model of the electrostatic trap with different electrodes in this 1T region. The focus of this study is primarily on the effect of potentials of electrodes A1 to A4, as these are important in creating the electrostatic trap that will hold the antiprotons for experimental purposes.

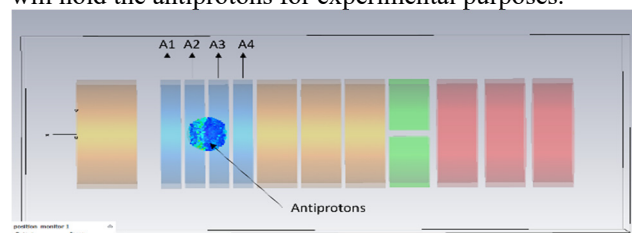


Figure 2: 3D model of electrostatic antiproton electrostatic trap.

The Particle-In-Cell (PIC)[6-8] technique has been widely used for studying fusion plasmas, laser wake field accelerations, gravitational systems etc. Using CST Studio, we create a 3D model of an electrostatic trap, solving Poisson's equation numerically to determine antiproton positions and velocities. The charge density is updated based on these positions, leading to the recalculation of the electric field in an iterative process. A constant 1T axial magnetic field is applied along the trap's centre axis to aid in antiproton confinement within the electrostatic trap.

The 10mm spherical source of the antiprotons is assumed to be at the centre of the electrostatic trap (i.e. centre of  $A_1$  and  $A_4$ ). The injection process of antiprotons into the trap itself is not simulated. The potentials on the end electrodes are kept  $V_{A1} = -14V$  and  $V_{A4} = -14V$  whereas the potentials on the inner two electrodes are varied simultaneously to create a potential well to trap the antiprotons. Different behaviour of antiproton dynamics can be studied under these varying conditions to select the best electrode configuration for trapping the antiprotons. For the present studies the simulation is run for  $100\mu s$  with  $\delta t \approx 1 \times 10^{-6}s$ . The initial temperature of the antiprotons is chosen to be around 55K and the number of macro particle simulated is around 1000 representing a density of around  $n = 1 \times 10^{12} m^{-3}$ . The mesh inside the simulation domain is chosen to be fine enough to resolve the antiproton motion. For observing the fluctuation in antiproton density, we define an observation plane at the centre of the electrostatic trap where we observe the variation of peak density of antiprotons, their mean energy and other parameters.

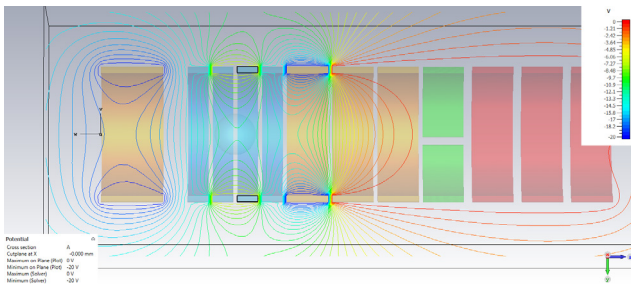


Figure 3: Electrostatic potential well with  $V_{A1} = V_{A4} = -14V$  and  $V_{A2} = V_{A3} = -7V$ .

## RESULTS AND DISCUSSION

Keeping the timesteps constant we vary the potentials of the inner electrodes A2 and A3 simultaneously to create a potential well as shown in Figure 3. By adjusting the potentials of the inner electrodes, the behaviour and density of antiprotons within the trap can be controlled. A higher potential for these inner electrodes, results in a shallower potential well. This scenario is depicted in Figure 4 (a), which illustrates the oscillations in peak antiproton density at the trap's centre plane ( $x, y = 0$ ) when the  $V_{A2}, V_{A3}$  potentials are varied from  $-12.4V$  to  $+5V$ . The average of the peak antiproton density remains constant for all values of inner electrode voltages as shown in Figure 4(b) whereas the average energy of the antiproton increases as the

potential well becomes steeper shown in Figure 4(c) due to stronger electric field.

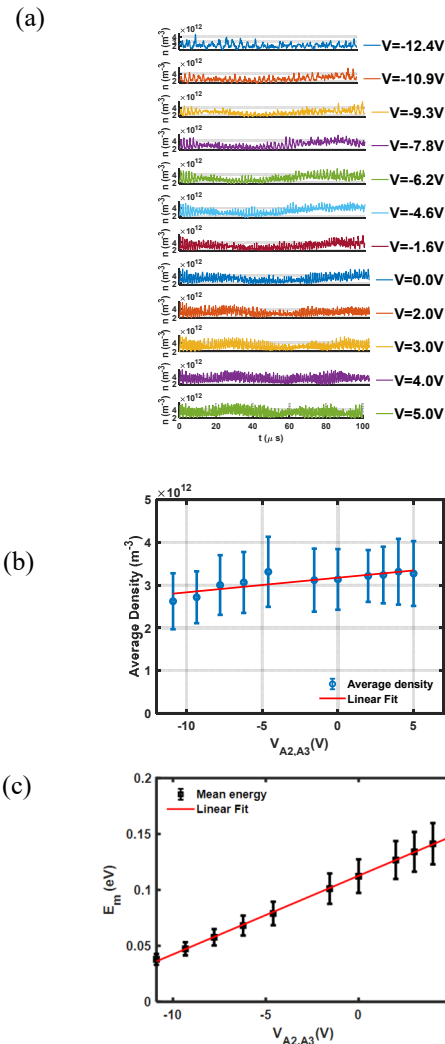


Figure 4: (a) 1D antiproton peak density variation as a function of time for different values of  $V_{A2}, V_{A3}$ . (b) Average density of antiprotons for different values of  $V_{A2}, V_{A3}$ . (c) Average energy of antiprotons for different values of  $V_{A2}, V_{A3}$ .

It is evident the peak density of antiprotons exhibits axial oscillations at a specific frequency. To investigate this, we conduct a FFT of the signal data obtained at the different voltage values. We find that the dominant axial oscillation frequency of the antiprotons varies as the function of the applied voltage depicted in Figure 5. In simplest one-dimensional case the axial oscillation frequency inside the penning trap is given by Eq.(1)[9].

$$f_{axial} = \frac{1}{2\pi} \sqrt{\frac{qV_0}{md^2}} \quad (1)$$

where,  $V_0$  is the potential different between centre of the trap to the outermost part of the trap,  $m$  is the mass of antiproton,  $d = 6.5mm$  is the distance between the centre of the trap to the inner edge of the outermost electrode.

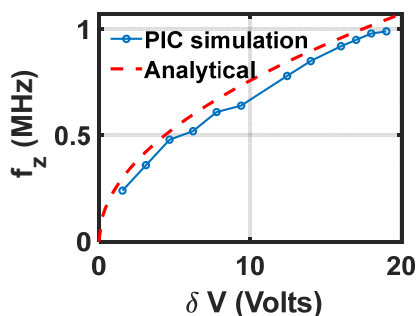


Figure 5: Comparison of analytical oscillation frequency and the frequencies derived from PIC simulations.

Figure 5 shows the comparison of the axial oscillation frequencies obtained from the PIC simulations and the analytical estimates obtained from Eq.1. The agreement between both the methods is within the acceptable limits which also validates the accuracy of the simulation. The slight discrepancies are probably due to space charge effects which are not included in the analytical formula.

Finally, we analyse the 1D density profiles over time for values of  $V_{A2}$ ,  $V_{A3}$  using the delayed coordinates embedding method [10] in two dimensional space. The delayed coordinates give the phase space representation of the 1D density profiles and can give some idea of the stability of the particles. In this technique the dynamics of the system can be reconstructed from the time series of a single observable by plotting it against delayed copies of itself. So, we plot the density of antiprotons  $N(t)$  against its delayed version  $N(t+\tau)$  where  $\tau$  is the time delay. Figure 6 shows the 1D antiproton density profile plotted in the delayed coordinates with  $\tau=1$  for  $V_{A2}$ ,  $V_{A3}=-12.44V$ . Red regions represent the states which are visited more frequently and could indicate more stable condition.

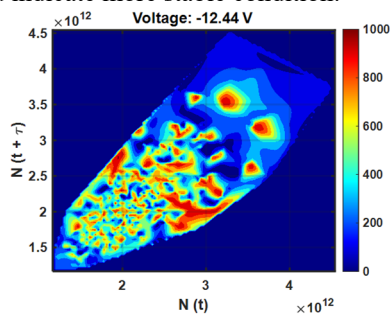


Figure 6: Phase space reconstruction of 1D density profile with delayed coordinates embedding with  $\tau=1$ .

Now we analyse the value of these stable regions for different values of potentials of the inner electrodes. In Fig.6 the horizontal axis represents the voltage applied at the inner electrode varying from negative to positive values. The vertical axis represents the time delay  $\tau$  used for constructing the delayed phase space. It indicates how the behaviour of the system evolves as the time delay increases. The colour coding indicates the sum of total areas from Figure 6 with values  $>950$ .

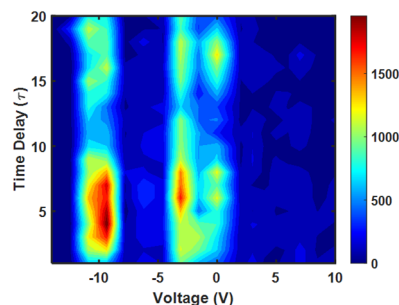


Figure 7: Maximum stable areas for different values of voltages ( $V_{A2}$ ,  $V_{A3}$ ) and time delays ( $\tau$ ).

The Figure 7 reveals distinct high-density zones, highlighted in red, where antiprotons exhibit repeated states. These regions mark the 'sweet spots' within the voltage spectrum that facilitate stable (repetitive states) trapping conditions. Notably, the plot suggests that negative voltage settings are more favourable for achieving regular and stable antiproton trapping. Specifically, one stable region is identified around  $-10V$ , and another, which is more pronounced, is found between  $-5V$  and  $0V$ . The persistence of these regions across various time delays ( $\tau$ ) demonstrates that the stability they signify is robust over time, not transient. Furthermore, while potentials greater than  $0V$  may form deeper potential wells, they exhibit more chaotic dynamics due to the lack of frequently recurring states. Operating the Penning trap at lower voltage levels is crucial as it results in smoother potential profiles, ensuring both the stability and the requisite low energy levels of antiprotons for the production of antihydrogen.

## CONCLUSIONS

The results of the 3D ES-PIC simulations indicate that the electrostatic trap exhibits zones of stable operation for trapping antiprotons effectively between  $-5V$  and  $0V$  and around  $-10V$ . These results would be critical for setting and operating conditions of the trap for experimental procedures that require a stable and cold population of trapped antiprotons. Further detailed analysis is necessary for understanding the closed loop, distinct clusters which may indicate more periodic motion whereas diffuse pattern might suggest more complex and chaotic behaviour. Additionally, the studies on presence of parabolic potential well extending from the 5T side to the 1T side could be pivotal for future research.

## REFERENCES

- [1] Caravita, R., et al., "The AEGIS experiment at CERN: Probing antimatter gravity", *Nuovo Cimento C-Colloquia and Communications in Physics*, 2019.42(2-3). doi:10.1393/ncc/i2019-19123-9
- [2] Caravita, R., et al., Towards a gravity measurement on cold antimatter atoms. *Nuovo Cimento C-Colloquia and Communications in Physics*, 2016. 39(1). Doi:10.1393/ncc/i2016-16237-6

- [3] G. Testera *et al.*, “The AEGIS experiment,” *Hyperfine Interact.*, vol. 233, no. 1–3, pp. 13–20, Mar. 2015. doi:10.1007/s10751-015-1165-5
- [4] E. K. Anderson *et al.*, “Observation of the effect of gravity on the motion of antimatter,” *Ann. Sci. Nat. Zool. Biol. Anim.*, vol. 621, no. 7980, pp. 716–722, Sep. 2023. doi:10.1038/s41586-023-06527-1
- [5] S. Maury *et al.*, “ELENA: the extra low energy anti-proton facility at CERN,” *Hyperfine Interact.*, vol. 229, no. 1–3, pp. 105–115, Apr. 2014. doi:10.1007/s10751-014-1067-y
- [6] T. D. Arber *et al.*, “Contemporary particle-in-cell approach to laser-plasma modelling,” *Plasma Phys. Controlled Fusion*, vol. 57, no. 11, p. 113001, Sep. 2015. doi:10.1088/0741-3335/57/11/113001
- [7] K. Matyash *et al.*, “Particle in Cell Simulation of Low Temperature Laboratory Plasmas,” *Contrib. Plasma Phys.*, vol. 47, no. 8–9, pp. 595–634, Dec. 2007. doi:10.1002/ctpp.200710073
- [8] Pukhov, A., “Particle-in-cell codes for plasma-based particle acceleration”, arXiv preprint arXiv:1510.01071, 2015. doi:10.48550/arXiv.1510.01071
- [9] K. Blaum, Yu. N. Novikov, and G. Werth, “Penning traps as a versatile tool for precise experiments in fundamental physics,” *Contemp. Phys.*, vol. 51, no. 2, pp. 149–175, Mar. 2010. doi:10.1080/00107510903387652
- [10] S. P. Garcia and J. S. Almeida, “Multivariate phase space reconstruction by nearest neighbor embedding with different time delays,” *Phys. Rev. E*, vol. 72, no. 2, Aug. 2005. doi:10.1103/physreve.72.027205